Name of Scientific area: MECHANICAL ENGINEERING

STRESS ANALYSIS TO THE OUTER FRAME OF A WHEELCHAIR

José Domingos Senra Simões, A65378@alunos.uminho.pt, Mechanical Eng. Student
Pedro Azevedo, A59436@alunos.uminho.pt, Mechanical Eng. Student
Rui Lopes, A61946@alunos.uminho.pt, Mechanical Eng. Student
Rui Barros, A66684@alunos.uminho.pt, Mechanical Eng. Student
Miguel Ferraz, A60283@alunos.uminho.pt, Mechanical Eng. Student
Paulo Cunha, A65420@alunos.uminho.pt, Mechanical Eng. Student
Pedro da Costa, A65391@alunos.uminho.pt, Mechanical Eng. Student
Eduardo Silva, A65406@alunos.uminho.pt, Mechanical Eng. Student
Andre Monteiro Fernandes, A65381@alunos.uminho.pt, Mechanical Eng. Student
Eurico Augusto Rodrigues de Seabra, eseabra@dem.uminho.pt, Mechanical Eng. Professor

ABSTRACT
The objective of the present article is to study a wheelchair in a way to lighten it and make it more comfortable to the user. For that, a structural analysis was carried out in order to study one component from the wheelchair.

The component that was chosen was the outer frame since it is one of the most important elements in the structure of the wheelchair. The outer frame is a structural element that supports the weight of the user, and contributes to the structural rigidness and stability of the wheelchair.

Since the structural analysis of the component is the objective of this article, static and fatigue studies were carried out. For each study, static and fatigue, there was an analytical and numerical analysis. Later with basis on the results obtained from the static and fatigue studies, there was a comparison between the analytical and the numerical analysis of each. With regard to the analytical analysis, the study was performed with basis on bibliography which pertained to the study. With regard to the numerical analysis, the study was performed with the help of computer software namely *SolidWorks*®.

KEYWORDS
Stress Analysis, Solidworks, Wheelchair

1 INTRODUCTION

The aim of this study is to analyze the mechanical behavior of a component of a manual folding wheelchair (Meyer, 1985), this study which will be carried out using analytical and numerical methods. The article consists essentially of the structural analysis of a wheelchair component subject to stress in a particular situation during the wheelchairs' life cycle (Boninger,2000). The wheelchair, despite already being used since the dawn of humanity, its evolution was slow compared to other areas related to health and mobility.

Boninger et all performed various structural analysis on wheelchairs (Boninger,2000), the one presented here lies on only one wheelchair component, a lateral support structure. This support gives rigidity to the structure, supports the user's weight and suffers point loads at the ends when a second person exerts a force on this rear bar to raise the front end of the chair, allowing the user to overcome obstacles, stairs, ledges or slopes.

The calculation of the damage caused by the forces on the component is obtained by analytical calculations and 3D modeling software and numerical simulation. The obtained results are compared allowing to conclude if they mutually confirming or, on the contrary, differ both in the type of stress and in their intensity.
This article focuses only on a wheelchair component, objective of the *Integradora IV* project of the MSc in Mechanical Engineering from the University of Minho, entitled "Moby Easy".

2 NOMENCLATURE

N = Safety Factor
D = Outer Diameter = 21.3 mm
d = Internal Diameter = 16.7 mm
α = 22.432o
CZ3 = 138.3 mm
AZ1 = 65.86 mm
AB = 202.6 mm
BC = 255.73 mm
DC = 155 mm
DE = 185 mm
EZ2 = 82.5 mm
CF = 415 mm
F2 = 2F1

3 STATE OF ART

Although the date of the appearance of the wheelchair is difficult to accurately determine, there is evidence suggesting the coexistence of chairs and wheels dating back to 4000 BC. However, the first test of this combination is visible in a Chinese illustration dating from the year 525 (Braga). During the following centuries, the improvements of the chairs were minimal, but a significant improvement occurs in the year 1655, when the German Stephan Farfler created the first chair with manual and autonomous propulsion, i.e. without the help of another individual. Two cranks were allowed as a manual override (Fig. 1) (chairdex).

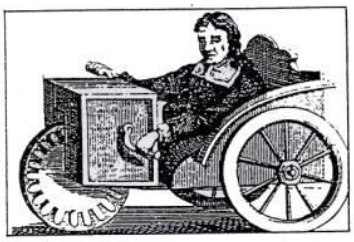

Fig. 1 - Stephan Farfler's Wheelchair

In 1811 progress in the mechanical area advance creating a chair with propulsion cranks with leg supports that tilt and swivel. In 1916, British engineers produced the first motorized wheelchair. 1932 is marketed by Everest & Jennings Company's first folding wheelchair, which will initiate an innovation race in the field of wheelchairs, this race is still going today. The emergence of new materials such as polymers and composite materials, the rise in requests for chairs and the development of sport for the disabled, allowed the successive increase in the quality and comfort of wheelchairs (Recherche).

4 METHODOLOGY

The structural analysis was divided into an analytical and a numerical structural analysis. With the knowledge in Material Mechanics it was possible to perform the necessary calculations for the resolution of our analytical analysis. For the numerical analysis, the finite element method in "SolidWorks®" was used to obtain the results. Lastly, the obtained results in both cases were compared to check for consistency.

4.1 FRACTURE

The failure by fracture is defined as a solid separated into two or more parts. This failure has two stages, first a fracture development stage and the next, the propagation of the fracture.

There are two types of fracture failures, these are fragile and ductile. The first is characterized by a sudden appearance, this appearance is caused by the release of a large amount of energy in a short time interval. This combination of events causes a rapid progression of the existing fracture in the material until it reaches a critical size. In this type of fracture, plastic deformation is greatly reduced. This type of fracture is quite catastrophic, since the existing residual strength in a structure with this type of fracture is quite low.
Since ductile fracture is characterized by a high degree of plastic deformation, which will lead to the occurrence of a slow propagation, thereby allowing its early detection.
With regard to the causes of brittle fracture, this may be caused by three factors:

- A triaxial stress state;
- Low temperatures;
- Very high loading speed or deformation.

The differences between the brittle and ductile fracture not only relate to the macroscopic analysis of the stress-strain curve, but also to the microstructural mechanisms. The fracture mechanisms are closely related to the crystallographic planes and are called cut and cleavage. The cutting mechanism is caused by some crystallographic slip planes, especially those where the shear strains are maximum, thus presenting as in ductile fracture, a local plastic deformation. Although, cleavage that occurs in different crystallographic planes, originates from a normal tensile stress and has a local plastic deformation greatly reduced. It should also be mentioned that the temperature of the material is very important in the type of fracture that a component can suffer. (Da Rosa)
Some traditional fracture tests:

- Fragile
    - Impact bending
    - Charpy
    - Izod
- Ductile
    - Slow Flexion
    - Robertson

4.2 FATIGUE

Fatigue is a phenomenon of progressive weakening and located in a material when it is subjected to dynamic or repeated loads (DeWolf). A sequence of fatigue damage can be broadly classified in the following stages: nucleation of the slot, microscopic growing crack, crack propagation and final breakage (Fitzgerald, 2001).

There are several types of fatigue in particular, mechanical fatigue (existence of cyclic stresses caused by external forces statically or cyclically) (Cooper,1996); thermal fatigue (thermal stresses due to excessive drops or sudden temperature rises along the component's lifetime); thermomechanical fatigue (simultaneous existence of thermal and mechanical fatigue); Fatigue with wear (characterized by the presence of tangential contact forces between two materials, in relative moving parts, giving rise to tangential tensile stresses) (Cooper,1996); fatigue contact (characterized by the existence of compressive stresses in the contact zone of components, water / oil fatigue (due to the oil/water pressure) and finally abrasion fatigue (characterized by the presence of particles between components in relative movement) (DeWolf).

There are two design philosophies to fatigue, guaranteed life and subsidiary life (Fitzgerald, 2001). Guaranteed assumes that the component has infinite life, or at least to last the allotted time, there is not supposed to be any concern or component inspection when projected for guaranteed life, stress and deformation analysis are included in this calculation. Controlled life assumes control of the evolution of the damage, it is supposed to know the parameters that control the development of cracks, and analysis based on fracture mechanics themselves encompasses this design philosophy (DeWolf).

The types of fatigue present in the wheelchair are mechanical fatigue, with wear and contact. The mechanical stress is present in the shaft of the wheelchair (Shimada, 1998), the existence of cyclical stresses caused by forces applied cyclically will cause this fatigue. Wear-fatigue is present virtually in the whole wheelchair (Cooper,1996), this fatigue is due to the tangential forces contact between two particular components with relative movement between them, these being the shaft and the wheels. Contact fatigue is present due to compression in the contact zone of the components.
The design philosophy used in the wheelchair is guaranteed life (Fitzgerald, 2001). This is the philosophy adopted because it is assumed that the chair has endless life or must last the allotted time, in other words, there should not be any concern or inspection throughout the lifetime.(DeWolf)

5 STRUCTURAL ANALYSIS ANALYTICAL

5.1 Fracture

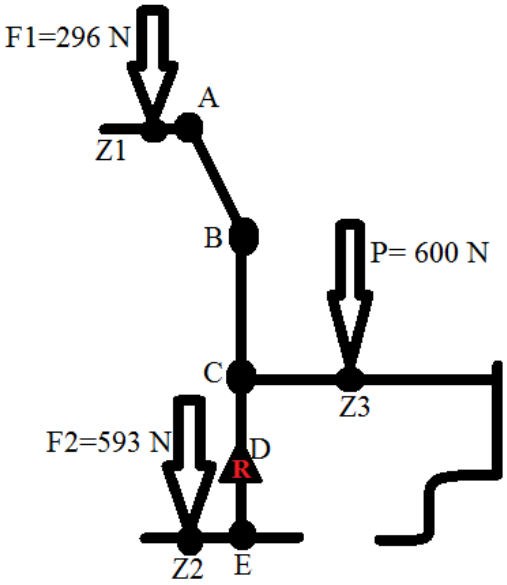

Fig. 2 - Free Body Diagram Component

Calculation of forces in Reactions

$$\sum MD<0$$
$$(600)*(CZ3) - F1*(AZ1+(Sin\alpha)*(AB)) - (F2)*(EZ2)<0$$
$$(600)*(CZ3) < F1*(AZ1+(Sin\alpha)*(AB) +(2)*(EZ2))$$

$$\frac{(600) * (138.3)}{2 * (82.5) + 65.86 + \mathrm{Sin}(22.432) * (202.6)} < F1$$

F1> 269.33 N
F2> 538.66 N

Adding 10% for the safety factor (safety factor = 1.1) we get:
F1=296 N; F2=593 N; R=1489 N.

To calculate the maximum stress we use the following expressions:

$$I = \frac{T*R^4}{4} \qquad \sigma_{max} = \frac{M_f}{W} \qquad W = \frac{\pi*(D^4-d^4)}{32*D}$$

so we get the final expression:

$$\sigma_{max} = \frac{M_f * 32 * D}{\pi * (D^4 - d^4)}$$

[Section A Z1]

$$\sigma_{max} = \frac{296 * 65.86 * 32 * 21.3}{\pi * (21.3^4 - 16.7^4)}$$
$$\sigma_{max} = 33.02 \text{ MPa}$$

[Section A B]

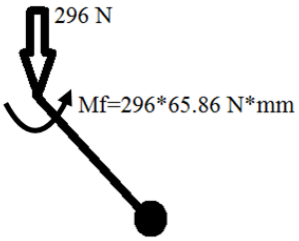

Fig. 3 - Free Body Diagram of the AB section.

$$F_H = \cos 22.432 \times F = 273.60 \text{ N}$$
$$F_V = \text{Sin } 22.432 \times F = 112.95 \text{ N}$$

Define the maximum bending moment:

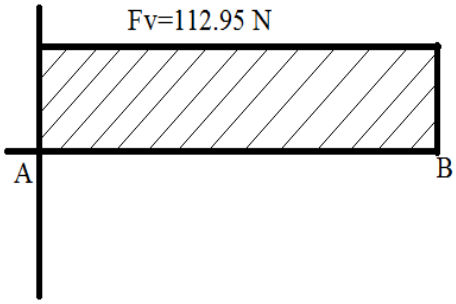

Fig. 4 - Efforts diagram (DeWolf)

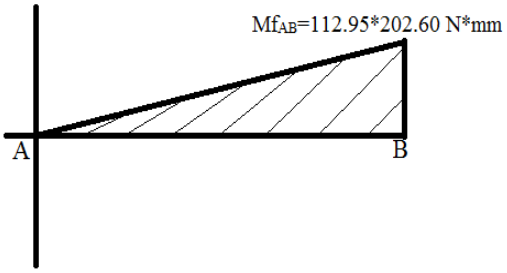

Fig. 5 - Bending Moments diagram (DeWolf)

We obtain the maximum bending moment due

$$M_{Res} = M_f + M_{AB}(\text{Boninger,1999})$$
$$M_{Res} = 42378.23 \text{ N} \times \text{mm} \text{ in section B}$$

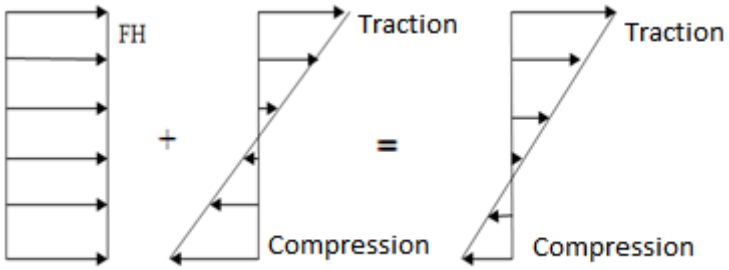

Fig. 6 - Diagram of tension / compression of the shaft AB (DeWolf)

Critical section is the lower section of the shaft AB B (compression)

$$\sigma_{Max\ AB} = \sigma_{Comp.} + \sigma_{flexão}$$

$$\sigma_{Max\ AB} = \frac{F_H \times 4}{\pi \times (D^2 - d^2)} + \frac{42378.23 \times 32 \times 21.3}{\pi \times (D^4 - d^4)}$$

$$\sigma_{Max\ AB} = \frac{273.60 \times 4}{\pi \times (21.3^2 - 16.7^2)} + \frac{42378.23 \times 32 \times 21.3}{\pi \times (D^4 - d^4)}$$

$$\sigma_{Max\ AB} = 1.99 + 71.8 = 73.79\ MPa$$

[Section B C]

$$M_{f2} = 296 \times (AZ_1 + ABSin\ \alpha)$$
$$M_{f2} = 296 \times (65.86 + 202.6Sin\ 22.432)$$
$$M_{f2} = 42378.16\ Nmm$$

F causes compressive stresses

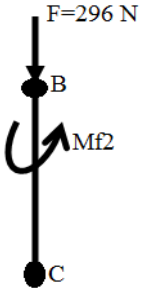

Fig. 7 - free body diagram of the BC bar (DeWolf).

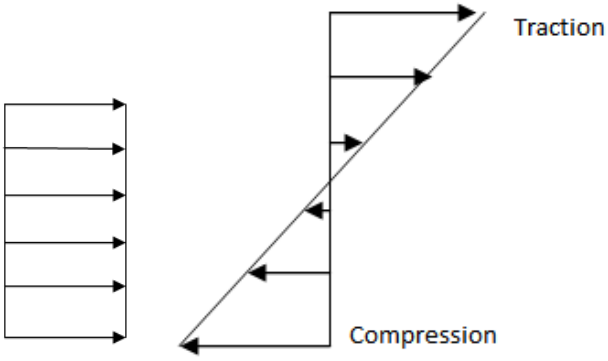

Fig. 8 - Traction / compression diagram of bar BC(DeWolf)

M_{f2} Promotes traction and compression.

Maximum stresses in BC in the "left" section C (where we have compression).

$$\sigma_{\text{Max BC}} = \sigma_{\text{Comp.}} + \sigma_{\text{flexão}}(\text{DeWolf})$$

$$\sigma_{\text{Max BC}} = \frac{F_H \times 4}{\pi \times (D^2 - d^2)} + \frac{42378.23 \times 32 \times 21.3}{\pi \times (D^4 - d^4)}$$

$$\sigma_{\text{Max BC}} = \frac{296 \times 4}{\pi \times (21.3^2 - 16.7^2)} + \frac{42378.23 \times 32 \times 21.3}{\pi \times (D^4 - d^4)}$$

$$\sigma_{\text{Max BC}} = 2.16 + 71.8 = 73.86 \text{ MPa}$$

[Section EZ_2]

$$F_H = \cos 22.432 \times F = 273.60 \text{ N}$$
$$F_V = \text{Sin } 22.432 \times F = 112.95 \text{ N}$$

Determination of the maximum bending moment:

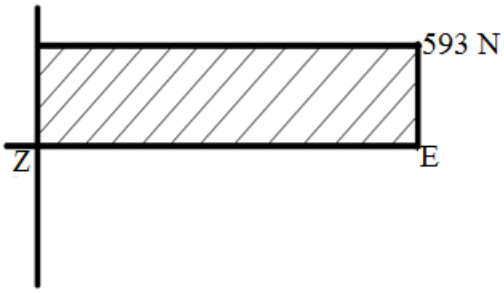

Fig. 9 - Efforts diagram(DeWolf)

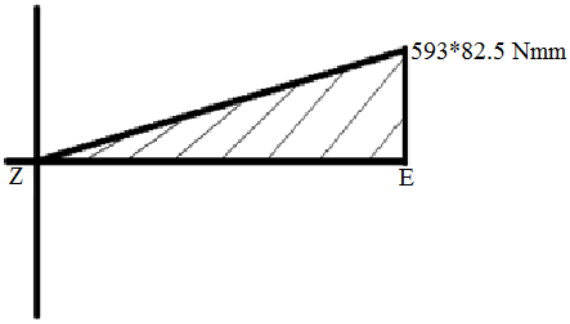

Fig. 10 - Bending Moment diagram(Boninger,1999)

We obtain the maximum stress with:

$$\sigma_{\text{Max EZ2}} = \frac{M_f}{W}$$

$$\sigma_{\text{Max EZ2}} = \frac{593 \times 82.5 \times 32 \times 21.3}{\pi \times (21.3^4 - 16.7^4)}$$

$$\sigma_{\text{Max EZ2}} = 82.89 \text{ MPa}$$

[Section E D]

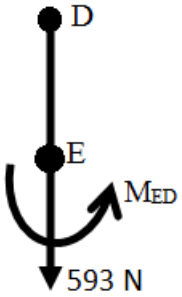

Fig. 11 - Free Body Diagram of bar DE.

Critical Section: Outer surface of the shaft on the left (under traction).

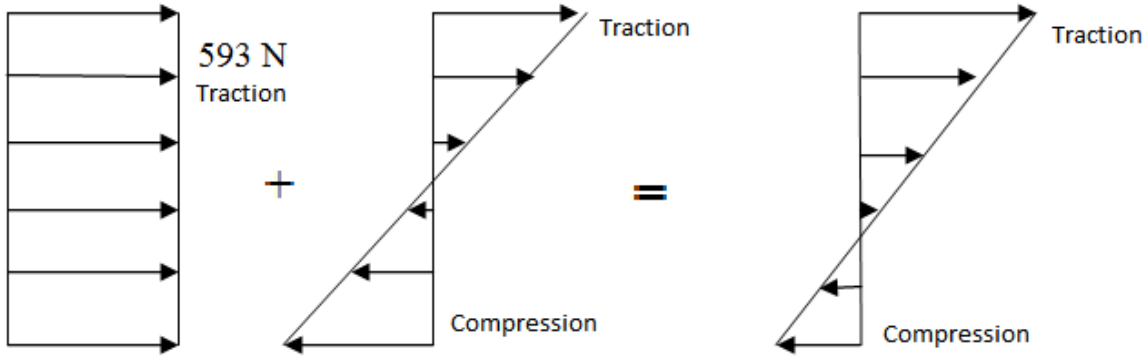

Fig. 12 - Diagram traction / compression of bar ED

$$\sigma_{\text{Max ED}} = \sigma_{\text{traction}} + \sigma_{\text{bend}}$$

$$\sigma_{\text{Max ED}} = \frac{F_2 \times 4}{\pi \times (D^2 - d^2)} + \frac{M_{ED} \times 32 \times D}{\pi \times (D^4 - d^4)}$$

$$\sigma_{\text{Max ED}} = 4.32 + 82.89 = 87.21 \text{ MPa}$$

The critical point is the outer surface of the shaft ED. Adopting the design criterion (for ductile metals)

$$\sigma_{\text{Max ED}} = \frac{\sigma_{\text{Cedencia}}}{N}$$

N= safety factor

It was determined the safety factor used in the design of ED bar.

$$87.0 < \frac{170}{N}$$

$$N < 1.95$$

So we can adopt a factor 1.1 to 1.9 and not have dimensioning problems. The bar is well dimentioned.

5.2 Fatigue

$$\sigma_R = 485\ MPa$$

$$\sigma_C = 170\ MPa$$

Component Studied: Bar Z2 E (Foot Bar)

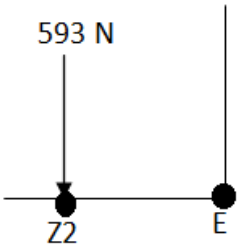

Fig. 13 - Free Body Diagram Bar Z2 E.

Critical Section: outside of the shaft in E (left, in traction)

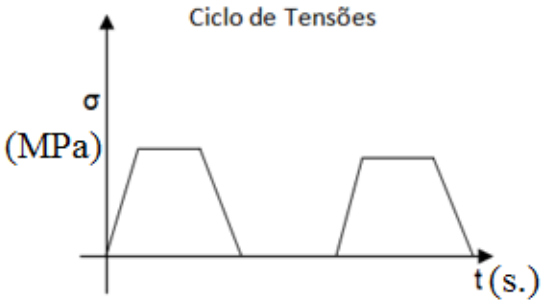

Fig. 14 - Stress Cycle Chart.

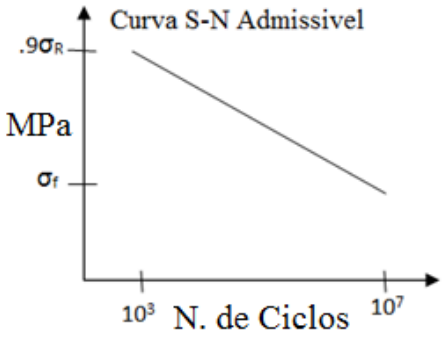

Fig. 15 - S N Curve Steel AISI 316L

$$\sigma_f = (k_s k_t k_f k_T) \times \frac{1}{K_f} \times \frac{1}{n} \times \sigma_{f0} \text{ (DeWolf)}$$

$$\sigma_{f0} = .5\sigma_R = 242.5 \text{ MPa (Steel with } \sigma_R < 1400 \text{ MPa)}$$

- n = 1.5
- Kf = 1 + q (kt-1) Cs = 1 + (. 75 (.75-1)). * 8 = .85
- kT = 1 (T <70 ◦C)
- kf = .868 (90% reliability)
- kt = .75 (d = 82.5 mm> 50 mm)
- ks = .8 (machined steel)$\sigma_f = \left(\frac{.8 \times .75 \times .868 \times 1}{.85 \times 1.5}\right) \times 242.5 \text{ MPa} = 99.05 \text{ MPa}$

Already determined that the maximum tensile stress due the repeated section of the foot loads has a value of 82.89 MPa.

The component has guaranteed life ($\sigma_{max} < \sigma_f$).

6 STRUCTURAL ANALYSIS IN SOLIDWORKS

6.1 Fracture

The fracture simulation was performed in SolidWorks ® motion study. Ferguson et al used a pressure mapping system to help with patient weight distribution (Ferguson,1993), in this case it is assumed that the patient weight is a point charge. The frame is fixed in the rear axle area and two forces are applied to the frame. The first force is also considered a point charge and is placed at the handle where a person would be pressing to tilt back the wheelchair. The second force, also a point charge is at the bottom of the frame where a person would press down with the foot to help with the tilting movement. Below, figure 18, shows the different pressure gradients in the frame and the corresponding values, all obtained from the simulation.

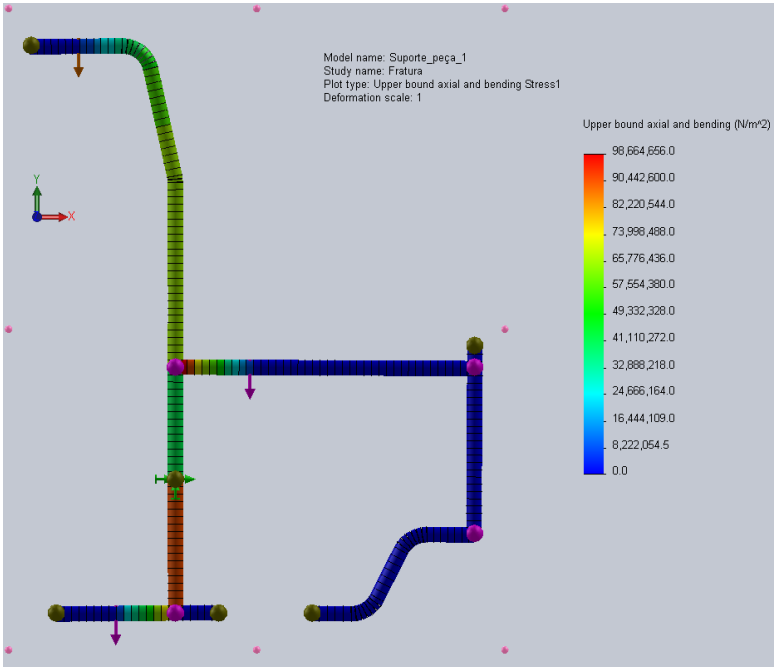

Fig. 16 - Print Screen of Stress Analysis in SolidWorks®.

Stresses in bars:

- Z1 A = 34.6 MPa
- A B = 69.4MPa
- B C = 69.4MPa
- D E = 87.2 MPa
- Z2 E = 82.8 MPa
-

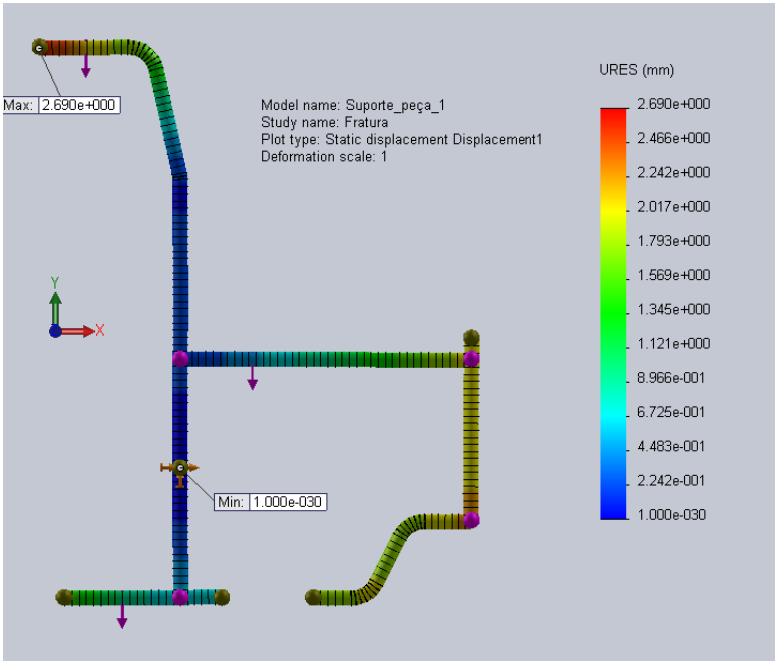

Fig. 17 - Print Screen of Deformation Analysis in SolidWorks®

Deformations in the bars:

- Z1 A = 1.7 mm
- A B = 0.2 mm
- B C = 0.2 mm
- D E = 0.5 mm
- Z2 E = 0.6 mm

6.2 Fatigue

It is possible to calculate the component cycles or if the component has infinite life through the SolidWorks® program, but in this case it was not possible because there is no available knowledge and the SolidWorks® does not have the SN curve of material in which the component is made of, AISI 316L steel. If there was more knowledge and experience there are ways for the user to enter and define the curve points for the simulation.

7 CONCLUSIONS

In this article, the structural study of a specific piece of a wheelchair was made, this study was based on the comparison of analytical and numerical analysis of these stresses in the part, considering a scenario in which the wheelchair (Van Der Woude, 1986) user is being pushed / picked up by a second person. These analyses were performed analytically and numerically with the help of SolidWorks® software. In this study it was concluded that both analyses showed identical values which leads to the conclusion that the seat is dimensioned well. However, a third analysis is pending due to lack of resources that the group offers, this is the experimental analysis, and this analysis would conclude that the analyses correspond to reality.

8 References

- Braga De Souza, Juarez Benicius, and Manuel Salomon Salazar Jarufe. *Concepção Da Estrutura Do Sistema Tecnológico De Uma Cadeira De Rodas Inteligente Adaptada Ao Utilizador*. Tech. Comp. Paula Alexandra Gomes Da Silva. Porto: FACULDADE DE ENGENHARIA DA UNIVERSIDADE DO PORTO, 2011. Print.
- Boninger, Michael L., Mark Baldwin, Rory A. Cooper, Alicia Koontz, and Leighton Chan. "Manual Wheelchair Pushrim Biomechanics and Axle Position." *Archives of Physical Medicine and Rehabilitation* 81.5 (2000): 608-13. *Science Direct*. Elsevier Inc, 23 Jan. 2004. Web.
- Boninger, Michael L., Rory A. Cooper, Mark A. Baldwin, Sean D. Shimada, and Alicia Koontz. "Wheelchair Pushrim Kinetics: Body Weight and Median Nerve Function." *Archives of Physical Medicine and Rehabilitation* 80.8 (1999): 910-15. *Science Direct*. Elsevier Inc., 25 May 2004. Web.
- "Chairdex - Wheelchair Resources." *Chairdex - Wheelchair Resources*. N.p., n.d. Web. 06 Apr. 2013.
- Cooper, Rory A., Rick N. Robertson, Brad Lawrance, and Tom Heil. "Life-cycle Analysis of Depot versus Rehabilitation Manual Wheelchairs." *Journal of Rehabilitation Research and Development* 33.1 (1996): 45-55. *ProQuest*. Web.
- Da Rosa, Edison. *Analise De Resistencia Mecanica- Mecanica Da Fratura E Fadiga*. Tech. N.p.: UFSC, 2002. Print.
- De Wolf. *Sebenta De Mecanica Dos Materiais*. Trans. Filipe Samuel. N.p.: n.p., n.d. Print.
- Ferguson, Martin Pell, and Mary D. Cardi. "Prototype Development and Comparative Evaluation of Wheelchair Pressure Mapping System." *Assistive Technology: The Official Journal of RESNA* 5.2 (1993): 78-91. *Taylor and Francis Online*. PubMed, 22 Oct. 2010. Web.
- Fitzgerald, Shirley G., PhD, Rory A. Cooper, PhD, Michael L. Boninger, MD, and Andrew J. Rentschler, BS. "Comparison of Fatigue Life for 3 Types of Manual Wheelchairs." *Archives of Physical Medicine and Rehabilitation* 82.10 (2001): 1484-488. *Science Direct*. Elsevier Inc., 9 May 2002. Web.
- Meyer, Bruno. Collapsible Wheelchair and Wheelchair Structure. Valutec Ag, assignee. Patent US 4684149 A. 21 May 1985. Print.
- "Recherche Sur Le Site." *CERAHTEC*. N.p., n.d. Web. 06 Apr. 2013.
- Shimada, Sean D., PhD, Rick N. Robertson, PhD, Michael L. Boninger, MD, and Rory A. Cooper, PhD. "Kinematic Characterization of Wheelchair Propulsion." *Journal of Rehabilitation Research and Development* 35.2 (1998): 210-18. *ProQuest*. Web.
- Van Der Woude, L.H.V., G. De Groot, A. P. Hollander, G. J. Van Ingen Schenau, and R. H. Rozendal. "Wheelchair Ergonomics and Physiological Testing of Prototypes." *Ergonomics* 29.12 (1986): 1561-573.*Taylor and Francis Online*. 30 May 2007. Web.